Biochemistry & Physiology: Open Access

Petit, Biochem Physiol 2013, S2
DOI: 10.4172/2168-9652.S2-006

Research Article Open Access

Fast Side-Chain Dynamics: Measurement, Analysis, and Their Role in Protein Function

Chad M Petit*

Department of Biochemistry and Molecular Genetics, University of Alabama at Birmingham, USA

Abstract

Proteins are dynamic molecules that use coordinated atomic fluctuations to achieve proper function. These motions have fundamental implications for not only understanding how proteins function, but current methods of structure based drug design. In this review, we focus on providing an overview of the NMR experiments used to detect side-chain motions and how they are applied to characterize to conformational entropy, allostery, and proper protein function.

Keywords: Entropy, Proteins, Spin relaxation, NMR

Introduction

Proteins in solution are not static entities but are "kicking and screaming stochastic molecules" that depend on the coordination of atomic motions to function properly [1]. These motions occur over a large range of timescales [2,3], from bond vibrations on the picosecond time scale to the folding and unfolding of biomolecules that may take seconds or longer (Figure 1). While there have been many techniques developed to explore how these motions affect and sustain biological processes, NMR is a powerful technique that offers many advantages over others. Perhaps, the biggest advantage NMR offers is that it allows experimental examination of protein motions over a wide range of time scales, with atomic resolution. NMR has shown that biological processes such as conformational switching and catalysis are dependent on motions occurring on the microsecond to millisecond (μs-ms), often called "slow", timescale [4-6]. However, not all proteins undergo significant motions on the slow timescale. In contrast, motions on the picosecond to nanosecond (ps-ns), often called "fast", timescale occur in all proteins, many of which result from fluctuations of backbone and side-chain dihedral angles. This review focuses on how the fast side-chain motions of methyl bearing residues are characterized using NMR and the effect these motions have on protein function.

The generalized order parameter, S^2, is a rigidity parameter that represents the internal re-orientational freedom of a given bond vector on the ps-ns timescale [7,8]. S^2 ranges from 0, corresponding to no favored position of the bond vector in the molecular frame, to 1 which corresponds to complete rigidity of the bond vector. For protein dynamics, order parameters are typically measured for a given bond vector, using NMR spin relaxation experiments. The most common bond vector motions measured are for backbone amide and side-chain methyl groups. As backbone amide order parameters provide information on site specific motions involving the main chain of the protein, the distribution of amplitudes of motion is relatively narrow throughout the protein for well folded and compact proteins. Conversely, side-chain order parameters, whose amplitudes are largely independent of secondary structure, vary considerably throughout the protein (Figure 2). What influences side-chain mobility is largely uncertain, as the amplitude of side-chain motions appear not to be correlated with packing density, depth of burial, or solvent accessible surface area [9]. However, a recent study by Fu et al. [10] used high pressure NMR to offer the intriguing idea that amplitudes of side-chain motions may be dictated by variations in the internal compressibilities of proteins. What is clear is that this variability facilitates modulation of protein activity and, therefore, makes obtaining information regarding side-chain motions indispensable to anyone interested in the motions of proteins.

Recently, there have been a number of high impact studies that highlight the role(s) that ps-ns methyl dynamics play in the free energy of binding *via* conformational entropy [11], as well as allosteric regulation of protein function [12]. As more systems that utilize these motions to regulate protein function are discovered, the biological relevance of ps-ns side-chain motions is becoming increasingly clear. Indeed, a recent study by Law et al. [13] suggests that side-chain dynamics may be as well conserved as primary sequence. This review seeks to provide an overview of how side chain dynamics are measured and analyzed using NMR, as well as notable systems in which they play an important role in function. For more in-depth considerations regarding ^{15}N (backbone) and ^{2}H (side-chain) relaxation theory and analysis, readers are referred to reviews by Jarymowycz and Stone [14] and Igumenova et al. [9], respectively.

From Spin Relaxation to Protein Dynamics

Nuclear spin relaxation experiments allow protein dynamics on the ps-ns time regime to be measured by NMR. In these experiments, a series of radio frequency pulses are used to perturb nuclear spins away from their ground state (Figure 3a). Their "relaxation" back to equilibrium can be monitored as a function of time to obtain relaxation rates. There are two types of relaxation processes which excited nuclei are subject to: transverse relaxation and longitudinal relaxation. Transverse relaxation is the dephasing of coherent magnetization as it precesses against a static magnetic field in the x-y plane. Longitudinal relaxation is the regeneration of the equilibrium Boltzmann population by the return of bulk magnetization along the static magnetic field. Relaxation processes are not spontaneous; instead they are stimulated

***Corresponding author:** Chad M Petit, Department of Biochemistry and Molecular Genetics, University of Alabama, 720, 20thStreet South, Kaul Human Genetics, Room 452, Birmingham, AL 35294, USA, E-mail: cpetit@uab.edu

Received February 06, 2013; **Accepted** May 13, 2013; **Published** May 16, 2013

Citation: Petit CM (2013) Fast Side-Chain Dynamics: Measurement, Analysis, and Their Role in Protein Function. Biochem Physiol S2: 006 doi:10.4172/2168-9652.S2-006

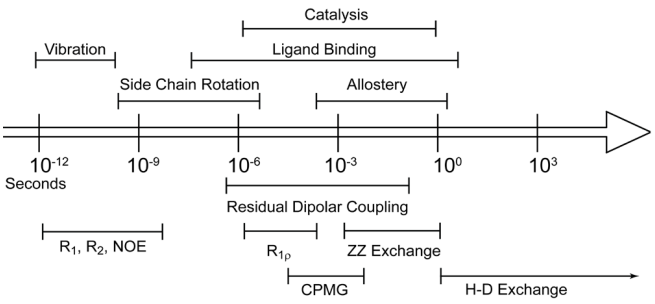

Figure 1: Motions in proteins associated with function and their respective timescales along with NMR experiments that offer insight into these motions.

The time scale of protein dynamics are represented by the center arrow, the types of motions associated with a given time scale are indicated above the time scale arrow, and NMR experiments that can be used to provide insight for a given time scale are indicated below the time scale arrow.

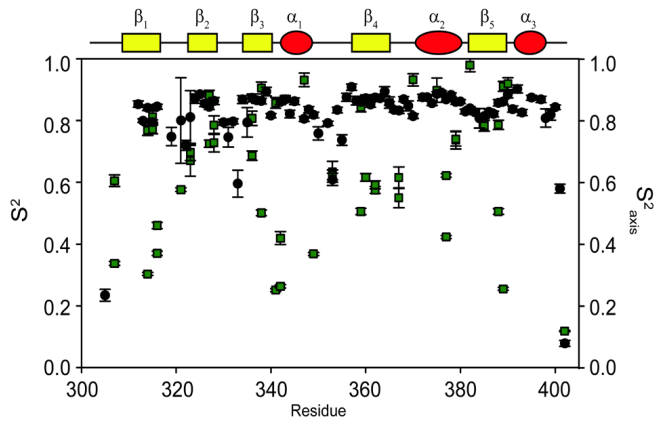

Figure 2: Backbone and side-chain methyl order parameters measured for PDZ3 [43].

Side-chain methyl order parameters, S^2_{axis}, are denoted by green squares whereas backbone order parameters, S^2, are denoted by black circles. The secondary structure of PDZ3 is represented on top of figure with red ovals depicting α-helices and yellow rectangles depicting β-sheets.

by local magnetic field fluctuations at or near the Larmor frequency of the target nucleus. Because the fluctuation of the local magnetic field is caused by molecular rotational motion, relaxation experiments can be utilized to yield information on the motions of bond vectors from spin relaxation measurements.

Measuring Spin Relaxation with NMR

For biomolecules, spin relaxation rates can be measured using a series of 2D heteronuclear single quantum coherence (HSQC) type experiments (Figure 3b), where each HSQC in the series utilizes a different relaxation time delay (T). During this relaxation time delay, molecular motions stimulate spin relaxation which results in modulation of peak intensities. By plotting the change in peak intensity as a function of relaxation delay, relaxation rates can be obtained by fitting a single exponential to the observed decay (Figure 3c). In 1995, Muhandiram et al [15] published the original set of pulse sequences designed to measure the D_z (longitudinal) and D_y (transverse) relaxation rates of ^{2}H nuclei. These pulse sequences are based on constant-time ^{1}H-^{13}C HSQC experiments and are fully detailed in Muhandiram et al [15]. Briefly, biomolecules are expressed in minimal media composed of ~60% D_2O/~ 40% H_2O supplemented with $^{15}NH_4Cl$ and ^{13}C-glucose as the sole nitrogen and carbon sources, respectively. These conditions allow methyl groups to be composed of a mixture of isotopomers (i.e. $^{13}CH_2D$ and $^{13}CHD_2$ where D is deuterium). Pulse sequences used to measure ^{2}H relaxation rates select for signals that originate from the $^{13}CH_2D$ isotopomer, with the degree of ^{2}H relaxation encoded in the intensity of ^{1}H-^{13}C HSQC resonances. The relaxation rates are then, in turn, used to fit the model free spectral density function to determine generalized order parameters specific for the methyl symmetry axis.

There have since been several modifications and improvements made to the original pulse sequences. In the original publication, a set of three experiments were necessary to obtain pure D_z or D_y relaxation rates. Briefly, the original pulse sequences measure triple spin coherences $I_zC_zD_z$ and $I_zC_zD_y$, where I=^{1}H, C=^{13}C and D=^{2}H. It was therefore, necessary to run an addition experiment that measures the contribution of the I_zC_z component in order to yield pure D_z or D_y relaxation rates. However, Millet et al. [16] have updated the original pulse sequences to subtract this component within each D_z or D_y experiment itself, making it unnecessary to collect a third data set. The use of transverse relaxation optimized spectroscopy (TROSY, [17]), as well as experiments that measure ^{1}H cross correlation relaxation [18], have also been developed to obtain order parameters for large molecules and protein complexes. These pulse sequences, along with new isotopic labeling schemes [19-21], allow the characterization of ps-ns methyl motions in proteins that were previously considered too large for NMR analysis.

There are multiple mechanisms by which motions on the ps-ns timescale can relax excited nuclear spins back to their ground state. Each mechanism's total contribution to the overall relaxation process

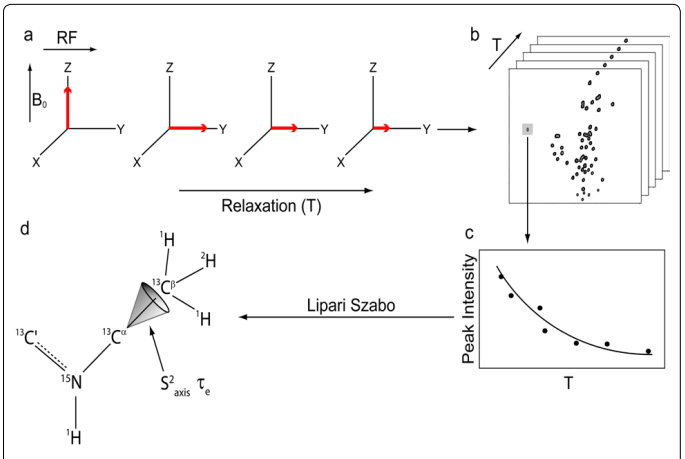

Figure 3: Schematic diagram outlining steps for obtaining methyl order parameters. (a) A graphical representation of D_y, or transverse, relaxation.

The static magnetic field (B_0) is indicated by a black vertical arrow, the radio frequency pulse applied is shown as a horizontal arrow labeled RF, and bulk magnetization is indicated by a red arrow. Following the radio pulse, the coherent magnetization is rotated into the x-y plane, where it precesses around B_0 and immediately begins to dephase. This loss of coherence indicated by a red arrow is a function of the relaxation time (T). (b) ^{2}H Relaxation is monitored by acquiring multiple 2D ^{1}H-^{13}C HSQC spectra with different relaxation times, thereby capturing magnetic relaxation at different points in its exponential decay curve. (c) To obtain ^{2}H D_z and D_y relaxation rates, peak intensities are measured as a function of relaxation time and fit to a single exponential. (d) The relaxation parameters are subsequently fit to the Lipari-Szabo model-free formalism to obtain methyl dynamic parameters that describe the amplitude (S^2_{axis}), and the characteristic time (τ_e) of the C-CH_3 symmetry axis.

typically depends on the type of nucleus being analyzed, along with the strength of the static magnetic field. Although there are many nuclei that are used for biomolecular NMR spectroscopy, this review will focus on the ^{2}H nucleus, as it is typically used to measure side-chain dynamics. Nuclei with I>1/2, e.g. ^{2}H, possess a nuclear electric quadrupole moment that interacts with local oscillations in the surrounding electric field gradients, thereby stimulating relaxation for excited spins. These interactions are highly effective at promoting relaxation, exceeding relaxation caused by other mechanisms by 1 to 2 orders of magnitude. Therefore, quadrupolar relaxation is the dominant relaxation mechanism for ^{2}H spins, making relaxation rates easily fit and interpretable. The ^{2}H nucleus has five independent operators or relaxation modes, with discrete relaxation rates that can linearly combined to describe the density matrix. The equations that describe these five independent relaxation modes are as follows [22]:

$$R^Q(D_z)=\frac{3}{16}\left(\frac{e^2qQ}{\hbar}\right)^2\left[J(\omega_D)+4J(2\omega_D)\right] \quad (1a)$$

$$R^Q\left(3D_z^2-2\right)=\frac{3}{16}\left(\frac{e^2qQ}{\hbar}\right)^2\left[3J(\omega_D)\right] \quad (1b)$$

$$R^Q(D_y)=\frac{1}{32}\left(\frac{e^2qQ}{\hbar}\right)^2\left[9J(0)+15J(\omega_D)+6J(2\omega_D)\right] \quad (1c)$$

$$R^Q(D_+D_z+D_zD_+)=\frac{1}{32}\left(\frac{e^2qQ}{\hbar}\right)^2\left[9J(0)+3J(\omega_D)+6J(2\omega_D)\right] \quad (1d)$$

$$R^Q\left(D_+^2\right)=R^Q\left(D_X^2+D_Y^2\right)=\frac{3}{16}\left(\frac{e^2qQ}{\hbar}\right)^2\left[J(\omega_D)+2J(2\omega_D)\right] \quad (1e)$$

where $\left(\frac{e^2qQ}{\hbar}\right)$, the quadrupolar coupling constant, is approximately 167 kHz [23] and $J(\omega)$ is the value of the spectral density evaluated at the indicated frequency (0, ω_D, $2\omega_D$). D_y (in-phase transverse magnetization), D_+D_z+D_zD_+ (antiphase transverse magnetization), and D_+^2 relaxation rates (double quantum magnetization) involve transitions between spin states, i.e. transverse relaxation, while D_z (longitudinal relaxation) and $3D_z^2$-2 relaxation rates (quadrupolar order) are related to the populations of spin states, i.e. longitudinal relaxation. These equations relate measured relaxation rates to the spectral density function, thereby providing a link between relaxation measurements and the frequency of molecular motions. It should be noted, however, that the measured relaxation rates report on the axially symmetric electric field gradient of the ^{2}H nucleus and not the ^{13}C-^{2}H bond vector of the side-chain methyl.

Model-Free Spectral Density Analysis

The most general approach to describe the reorientational motions of a bond vector is to define a time-dependent rotational autocorrelation function. When assuming a motional model of isotropic molecular tumbling with no internal motion, the function can be defined as follows:

$$C(t)=\frac{1}{5}e^{-t/-\tau_m} \quad (2)$$

where τ_m is the rotational correlation time. This correlation function is particularly useful when separating motions that occur on a variety of time scales, and forms the basis for simple parametric models of angular bond vector motion [14,24]. The spectral density function, J(ω), can be obtained through the Fourier transformation of C(t), and can be expressed as

$$J(\omega)=\frac{2}{5}\left(\frac{\tau_m}{1+(\omega\tau_m)^2}\right) \quad (3)$$

While this form of the spectral density function describes the relative amplitude of bond vector motion at a given frequency, it assumes a motional model with isotropic tumbling and no internal motions. Therefore, it cannot be used to distinguish molecular tumbling motions from internal protein dynamics. To separate the internal dynamics from the global motions, Lipari and Szabo [7,8] introduced a modified spectral density function that assumes no specific physical motional model. Known as the "model free" formalism, this modified spectral density function allows the isolation of internal motions from overall tumbling, by assuming that the internal dynamics of a protein are much faster than, and consequentially independent of, overall molecular tumbling. The model free spectral density function can be expressed as

$$J(\omega)=\frac{2}{5}\left(\frac{S^2\tau_m}{1+(\omega\tau_m)^2}+\frac{\tau\left(1-S^2\right)}{1+(\omega\tau)^2}\right),\ \tau^{-1}=\tau_m^{-1}+\tau_e^{-1} \quad (4)$$

where S^2 is the order parameter describing the degree of angular restriction for a given bond vector, τ_e represents the characteristic time of the bond vector motion, and τ_m is the rotational correlation time. For the majority of methyl groups, a single order parameter and correlation time is sufficient to describe local dynamics. However, a more detailed analysis of side-chain motions has been developed for residues that have additional, slower motions (i.e. low nanosecond), that are incompatible with the two-parameter model [16,25].

As noted above, there are certain assumptions that need to be made when using ^{2}H relaxation measurements to obtain information on the motions of the C-CH_3 symmetry axis of methyl side chains. These assumptions are necessary because the measured relaxation rates report on motions involving the principle axis of the electric field gradient tensor, not on the motions of the C-D bond vector that is of primary interest. Therefore, fitting ^{2}H relaxation data to the model free formalism yields order parameters for the principle axis of the electric field gradient tensor. The two assumptions that allow measured ^{2}H relaxation rates to be directly related to the biologically relevant motions of side chains are as follows: 1) The principle axis of the electric field gradient tensor is collinear with the C-D bond vector [23,26]. Because they are assumed to be collinear, the motions of the principle axis of the electric field gradient tensor are analogous to those of the C-D bond vector. 2.) The methyl group being analyzed has tetrahedral geometry. This condition allows the motions about the methyl symmetry axis to be separated from the motions of the symmetry axis itself. Although the rapid rotation about the axis is the primary motion of the C-D bond, it is not of primary interest for this review. By assuming that the methyl group has tetrahedral geometry, rotation about the axis can be removed from the S^2 parameter by using Equation 5 where θ_1 is the angle between the C-D bond and the averaging axis (109.5°) [15,23].

$$S^2=S^2_{axis}\left[\left(3\cos^2\Theta_1-1\right)/2\right] \quad (5)$$

S^2_{axis} therefore reports only on the motions of the methyl symmetry axis and not on motions about the methyl axis of rotation (Figure 3d). For τ_e, the characteristic time of motions about the methyl symmetry axis

cannot be sufficiently separated from the characteristic time of motions of the symmetry axis; therefore, τ_e reports on a combination of both dynamic processes. Although it is presently unclear how to robustly interpret τ_e, it does provide a sensitive probe for monitoring changes in protein dynamics upon perturbations such as mutation or the binding of a target ligand [27,28].

Functional Relevance

Atomic fluctuations, as measured by S^2, were first realized to have potential functional relevance when they were shown to be related to the Gibbs free energy equation [30]. An analytical relationship was then derived that linked order parameters measured by NMR to the local residual entropy of proteins [31,32]. While the relationship derived did not offer a reliable method for calculating absolute entropies from measured order parameters, it did provide a robust evaluation of relative entropic differences (e.g. differences between free and bound states). This relationship led to the hypothesis asserting that relative differences in order parameters could serve as a proxy for changes in conformational entropy, assuming the absence of correlated motions or, if present, the extent of these motions being the same in both states.

Methyl Order Parameters as a Proxy for Conformational Entropy

The prediction that differences in order parameters could serve as a proxy for changes in the conformational entropy was verified experimentally by Frederick et al. [33], using calmodulin as a model system. The entropic contribution measured calorimetrically can be deconstructed into several components associated with the protein, the ligand, and the solvent as follows:

$$\Delta G_{\text{bind}} = \Delta H_{\text{bind}} - \text{T}\Delta \text{S}_{\text{bind}} = \Delta H_{\text{bind}} - T(\Delta S_{\text{protein}} + \Delta S_{\text{ligand}} + \Delta S_{\text{solvent}}) \quad (6)$$

where ΔG_{bind} is the ΔG for a protein binding its target ligand. Both ΔS_{ligand} and $\Delta S_{\text{solvent}}$ are well established in the way they are able to affect the entropic contribution to biding free energy. What was less understood is the entropic contribution from the "structured" protein, which includes changes in its conformational, rotational, and translational entropy. Frederick et al. [33] selected calmodulin to further examine the relationship between the dynamics of side-chains and conformational entropy involved in binding. Calmodulin interacts and regulates a substantial number of proteins, allowing it to be an essential participant in calcium-mediated signal transduction pathways in eukaryotes [34,35]. Previous studies that monitored changes in fast side-chain motions upon ligand binding found a significant redistribution of these motions throughout the protein [36]. The question of whether this redistribution allows internal motions to "tune" affinity for different ligands, was a significant driving force for this study. Specifically, how is conformational entropy able to modulate the free energy of binding between a protein and its target ligand? To address this question, the dynamic response of calcium-saturated calmodulin (CaM) was monitored as a function of binding six peptides representing naturally occurring calmodulin binding partners. Backbone dynamics showed negligent variation across all complexes, indicating that they play no role in "tuning" binding affinity. However, the ps-ns motions of methyl-bearing side chains vary significantly with the type of target domain. The changes in methyl order parameters were then related to the conformation entropy by using a simple harmonic oscillator model [31]. Despite potential limitations of this method [9,33], the total binding entropy to the six peptides correlated linearly (R^2=0.78) with the corresponding apparent changes in conformational entropy, calculated by simple summation of the individual local entropies. This remarkable observation provided the first experimental evidence that order parameters measured by NMR could serve as a proxy for entropy associated with the binding free energy.

Entropic Modulation in a PDZ Domain

It has also been discovered that side chains can facilitate communication between sites that would not be suspected to be energetically linked based on their three dimensional structure alone [27,28,37-39]. Therefore, the ability of side changes to serve as a reservoir of conformational entropy, as well as to facilitate intramolecular communication, suggests that these motions may offer a foundation for allosteric communication without detectable conformational change. [40-43].

PDZ domains are small monomeric proteins often found in scaffolding proteins composed of modular structures that make up larger, multi-domained proteins. The third PDZ domain from PSD-95/SAP90 (PDZ3), a neuronal scaffolding protein, is commonly thought of as the archetype of PDZ domains. The PDZ family has a highly conserved fold that consists of a 6-stranded half β-barrel and 2 α-helices [44]. However, there are many examples of members of the PDZ superfamily that contain additional structural elements or varying lengths of loops, β-strands, or helices [45-49]. Although considered the archetype of the PDZ superfamily, PDZ3 contains an atypical third α-helix on its carboxyl terminus. This additional structural element is thought to be biologically relevant because it has been shown to be phosphorylated, *in vivo*, at position Y397 [50]. To investigate the effects of this modification on protein structure and dynamics, Petit et al. [43] constructed a 7 amino acid deletion mutant of PDZ3, referred to here as Δ7ct. Δ7ct was designed to mimic the undocking of the C-terminal helical extension of PDZ3 upon phosphorylation of Y397 [51]. The thermodynamic properties of PDZ3 and Δ7ct binding to a naturally occurring target peptide, CRIPT [52], were assessed by isothermal titration calorimetry. These measurements indicated that the binding affinity of Δ7ct to CRIPT is reduced by 21-fold from PDZ3, and that, remarkably, the difference between the two binding affinities is entirely due to the entropic component. As there was no evidence of gross structural changes that could explain this observed difference in binding affinity, relaxation experiments were employed to determine whether there were dynamic differences between the two constructs. Backbone dynamics revealed essentially no differences between the two constructs and, therefore, could not account for the observed variation in binding thermodynamics. A comparison of ps-ns side-chain motions of methyl containing residues, however, revealed global decreases in S^2_{axis} when compared to PDZ3. This global increase in flexibility is consistent with the increased entropic penalty paid upon CRIPT binding observed for Δ7ct. Indeed, the enhanced motions are quenched upon CRIPT binding with the Δ7ct bound complex, virtually mirroring the dynamic profile of the PDZ3 bound complex. It was, therefore, concluded that the additional entropic penalty observed for Δ7ct binding is due to increased motions (i.e. conformation entropy) in the side chains of the unbound protein. It is also worth noting that the dynamic changes occur throughout the protein, with a large number being distal to the binding pocket. These two points taken together, suggest that the changes in conformational entropy associated with side-chain dynamics, is the driving force behind the allosteric behavior observed in PDZ3.

Conformational Entropy, Not Structure, Modulates Binding in Catabolite Activator Protein

The way in which the interplay between the three dimensional structure of a protein and its internal dynamics serve to regulate protein function is poorly understood. We often cannot rationalize the effects that perturbations of proteins *via* mutation, post-translational modification, or ligand binding have on proper function solely on the basis of structural information. To help better understand the relationship between structure, dynamics, and function, Kalodimos et al. have published several studies using catabolite activator protein (CAP) as a model system [53-56]. CAP is a transcriptional activator that exists in solution as a homodimer, with a DNA binding domain at each monomer's carboxyl terminus and a ligand binding domain at each monomer's amino terminus [57,58]. Briefly, two cyclic AMP (cAMP) molecules bind to the cAMP-binding domain of CAP with negative cooperativity, allosterically inducing a reorientation of its DNA-binding domain (DBD). This structural reorientation switches CAP from an inactivated state that is incapable of binding DNA to an active state that binds DNA with high efficiency. In the most recent study, a series of allosteric mutants of CAP in the unliganded, cNMP-liganded, and DNA liganded forms are used to dissect the contributions from structure and internal dynamics to binding energetics [56]. It was first shown by NMR chemical shift analysis that the CAP variants demonstrated a predictable linear derivation connecting resonances corresponding to the apo, inactivated form of CAP to the cAMP bound, activated form of CAP. Each CAP variant's position relative to one another is indicative of the relative populations of inactive and active forms, with the average chemical shift resulting from the weighted fraction of the active and inactive populations [59-62]. Intuitively, the relative CAP binding affinity for DNA should correlate with the relative population of the active form of the protein. Namely, a CAP variant with a higher population of the active form of CAP should, in principle, have a higher binding affinity for DNA. Shockingly, this was found not to be the case with experimentally measured binding affinities showing no correlation with the relative population of the active form of CAP. This unexpected result demonstrated that the DNA binding affinity of CAP is modulated not primarily by structure but instead by another, then unknown, factor. Isothermal titration calorimetry was used to thermodynamically characterize each variant's energetic basis for binding DNA. The calorimetry data indicated that although the enthalpic contribution to binding free energy was remarkably consistent across all variants, the entropic contribution spanned a significant range of ~ 35 kcal mol^{-1}. Because spatial fluctuations that bond vectors undergo had been shown to be related to conformational entropy [29-33,43,63-65], the changes in S^2_{axis} values of the side-chain methyl groups upon DNA binding were determined for each variant. ^{1}H spin-based relaxation experiments were used [18] in place of the traditional ^{2}H-based relaxation experiments [66] as they are optimally suited for large protein complexes such as the CAP-DNA complex (~ 90 kDa). To assess the contribution of protein motions to binding conformational entropy ($-T\Delta S_{conf}$), changes in S^2_{axis} upon DNA binding were measured. These changes were then used to determine the conformational entropy of binding using the empirical calibration approach pioneered by Marlow et al. [63]. Remarkably, there was found to be a linear correlation between the total binding entropy, as measured by isothermal titration calorimetry, and the conformational entropy, as determined by changes in S^2_{axis}. This led to the conclusion that conformational entropy determines whether protein-ligand interactions will occur, even in cases where the ligand binding interfaces are structurally identical.

Conclusion

The evidence for ps-ns side chain motions being an essential element involved in proper protein function is steadily increasing. The notion that proteins exist as static, single structures is steadily giving way to the realization that proteins dynamically sample a myriad of substructures within the native ensemble. The more that is learned about how these sampled states affect protein function, the more effective structure based drug design will become. By considering both the structural and the dynamical aspects of proteins, we will gain a more comprehensive understanding of protein functionality.

Acknowledgments

We thank Anthony B. Law, Rene E. Gauthreaux, and Paul J. Sapienza for their discussions and review of the manuscript. We gratefully acknowledge financial support from the Department of Biochemistry and Molecular Genetics at UAB.

References

1. Weber G (1975) Energetics of ligand binding to proteins. Adv Protein Chem 29: 1-83.
2. Frauenfelder H, Sligar SG, Wolynes PG (1991) The energy landscapes and motions of proteins. Science 254: 1598-1603.
3. Onuchic JN, Luthey-Schulten Z, Wolynes PG (1997) Theory of protein folding: the energy landscape perspective. Annu Rev Phys Chem 48: 545-600.
4. Eisenmesser EZ, Bosco DA, Akke M, Kern D (2002) Enzyme dynamics during catalysis. Science 295: 1520-1523.
5. Eisenmesser EZ, Millet O, Labeikovsky W, Korzhnev DM, Wolf-Watz M, et al. (2005) Intrinsic dynamics of an enzyme underlies catalysis. Nature 438: 117-121.
6. Boehr DD, McElheny D, Dyson HJ, Wright PE (2006) The dynamic energy landscape of dihydrofolate reductase catalysis. Science 313: 1638-1642.
7. Lipari G, Szabo A (1982) Model-free approach to the interpretation of nuclear magnetic-resonance relaxation in macromolecules.1.Theory and range of validity. J Am Chem Soc 104: 4546-4559.
8. Lipari G, Szabo A (1982) Model-free approach to the interpretation of nuclear magnetic-resonance relaxation in macromolecules. 2. Analysis of experimental results. J Am Chem Soc 104: 4559-4570.
9. Igumenova TI, Frederick KK, Wand AJ (2006) Characterization of the fast dynamics of protein amino acid side chains using NMR relaxation in solution. Chem Rev 106: 1672-1699.
10. Fu Y, Kasinath V, Moorman VR, Nucci NV, Hilser VJ, et al. (2012) Coupled motion in proteins revealed by pressure perturbation. J Am Chem Soc 134: 8543-8550.
11. Wand AJ (2013) The dark energy of proteins comes to light: conformational entropy and its role in protein function revealed by NMR relaxation. Curr Opin Struct Biol 23: 75-81.
12. Tzeng SR, Kalodimos CG (2011) Protein dynamics and allostery: an NMR view. Curr Opin Struct Biol 21: 62-67.
13. Law AB, Fuentes EJ, Lee AL (2009) Conservation of side-chain dynamics within a protein family. J Am Chem Soc 131: 6322-6323.
14. Jarymowycz VA, Stone MJ (2006) Fast time scale dynamics of protein backbones: NMR relaxation methods, applications, and functional consequences. Chem Rev 106: 1624-1671.
15. Muhandiram DR, Yamazaki T, Sykes BD, Kay LE (1995) Measurement of H-2 T-1 and T-1p relaxation-times in uniformly C-13-labeled and fractionally H-2-labeled proteins in solution. J Am Chem Soc 117: 11536-11544.
16. Millet O, Muhandiram DR, Skrynnikov NR, Kay LE (2002) Deuterium spin probes of side-chain dynamics in proteins. 1. Measurement of five relaxation rates per deuteron in (13)C-labeled and fractionally (2)H-enriched proteins in solution. J Am Chem Soc 124: 6439-6448.
17. Pervushin K, Riek R, Wider G, Wüthrich K (1997) Attenuated T2 relaxation by mutual cancellation of dipole-dipole coupling and chemical shift anisotropy indicates an avenue to NMR structures of very large biological macromolecules in solution. Proc Natl Acad Sci U S A 94: 12366-12371.

18. Tugarinov V, Sprangers R, Kay LE (2007) Probing side-chain dynamics in the proteasome by relaxation violated coherence transfer NMR spectroscopy. J Am Chem Soc 129: 1743-1750.

19. Tugarinov V, Kanelis V, Kay LE (2006) Isotope labeling strategies for the study of high-molecular-weight proteins by solution NMR spectroscopy. Nat Protoc 1: 749-754.

20. Ayala I, Sounier R, Usé N, Gans P, Boisbouvier J (2009) An efficient protocol for the complete incorporation of methyl-protonated alanine in perdeuterated protein. J Biomol NMR 43: 111-119.

21. Sinha K, Jen-Jacobson L, Rule GS (2011) Specific labeling of threonine methyl groups for NMR studies of protein-nucleic acid complexes. Biochemistry 50: 10189-10191.

22. Jacobsen JP, Bildsoe HK, Schaumburg K (1976) Application of density matrix formalism in nmr-spectroscopy. 2. One-spin-1 case in anisotropic phase. J Magn Reson 23: 153-164.

23. Mittermaier A, Kay LE (1999) Measurement of methyl H-2 quadrupolar couplings in oriented proteins. How uniform is the quadrupolar coupling constant? J Am Chem Soc 121: 10608-10613.

24. Lee AL, Wand AJ (2001) In Els, John Wiley and Sons, Ltd, USA.

25. Skrynnikov NR, Millet O, Kay LE (2002) Deuterium spin probes of side-chain dynamics in proteins. 2. Spectral density mapping and identification of nanosecond time-scale side-chain motions. J Am Chem Soc 124: 6449-6460.

26. Lee AL, Flynn PF, Wand AJ (1999) Comparison of H-2 and C-13 NMR relaxation techniques for the study of protein methyl group dynamics in solution. J Am Chem Soc 121: 2891-2902.

27. Clarkson MW, Lee AL (2004) Long-range dynamic effects of point mutations propagate through side chains in the serine protease inhibitor eglin c. Biochemistry 43: 12448-12458.

28. Clarkson MW, Gilmore SA, Edgell MH, Lee AL (2006) Dynamic coupling and allosteric behavior in a nonallosteric protein. Biochemistry 45: 7693-7699.

29. Sapienza PJ, Lee AL (2010) Using NMR to study fast dynamics in proteins: methods and applications. Curr Opin Pharmacol 10: 723-730.

30. Akke M, Bruschweiler R, Palmer AG (1993) NMR order parameters and free-energy-An analytical approach and its application to cooperative Ca^{2+} binding by calbindin-D(9k). J Am Chem Soc 115: 9832-9833.

31. Li Z, Raychaudhuri S, Wand AJ (1996) Insights into the local residual entropy of proteins provided by NMR relaxation. Protein Sci 5: 2647-2650.

32. Yang D, Kay LE (1996) Contributions to conformational entropy arising from bond vector fluctuations measured from NMR-derived order parameters: Application to protein folding. J Mol Biol 263: 369-382.

33. Frederick KK, Marlow MS, Valentine KG, Wand AJ (2007) Conformational entropy in molecular recognition by proteins. Nature 448: 325-329.

34. Yap KL, Kim J, Truong K, Sherman M, Yuan T, et al. (2000) Calmodulin target database. J Struct Funct Genomics 1: 8-14.

35. Kahl CR, Means AR (2003) Regulation of cell cycle progression by calcium/calmodulin-dependent pathways. Endocr Rev 24: 719-736.

36. Lee AL, Kinnear SA, Wand AJ (2000) Redistribution and loss of side chain entropy upon formation of a calmodulin-peptide complex. Nat Struct Biol 7: 72-77.

37. Fuentes EJ, Der CJ, Lee AL (2004) Ligand-dependent dynamics and intramolecular signaling in a PDZ domain. J Mol Biol 335: 1105-1115.

38. Fuentes EJ, Gilmore SA, Mauldin RV, Lee AL (2006) Evaluation of energetic and dynamic coupling networks in a PDZ domain protein. J Mol Biol 364: 337-351.

39. Namanja AT, Peng T, Zintsmaster JS, Elson AC, Shakour MG, et al. (2007) Substrate recognition reduces side-chain flexibility for conserved hydrophobic residues in human Pin1. Structure 15: 313-327.

40. Cooper A, Dryden DT (1984) Allostery without conformational change. A plausible model. Eur Biophys J 11: 103-109.

41. Wand AJ (2001) Dynamic activation of protein function: a view emerging from NMR spectroscopy. Nat Struct Biol 8: 926-931.

42. Tsai CJ, del Sol A, Nussinov R (2008) Allostery: absence of a change in shape does not imply that allostery is not at play. J Mol Biol 378: 1-11.

43. Petit CM, Zhang J, Sapienza PJ, Fuentes EJ, Lee AL (2009) Hidden dynamic allostery in a PDZ domain. Proc Natl Acad Sci U S A 106: 18249-18254.

44. Doyle DA, Lee A, Lewis J, Kim E, Sheng M, et al. (1996) Crystal structures of a complexed and peptide-free membrane protein-binding domain: molecular basis of peptide recognition by PDZ. Cell 85: 1067-1076.

45. Morais Cabral JH, Petosa C, Sutcliffe MJ, Raza S, Byron O, et al. (1996) Crystal structure of a PDZ domain. Nature 382: 649-652.

46. Birrane G, Chung J, Ladias JA (2003) Novel mode of ligand recognition by the Erbin PDZ domain. J Biol Chem 278: 1399-1402.

47. Peterson FC, Penkert RR, Volkman BF, Prehoda KE (2004) Cdc42 regulates the Par-6 PDZ domain through an allosteric CRIB-PDZ transition. Mol Cell 13: 665-676.

48. Mishra P, Socolich M, Wall MA, Graves J, Wang Z, et al. (2007) Dynamic scaffolding in a G protein-coupled signaling system. Cell 131: 80-92.

49. Bhattacharya S, Dai Z, Li J, Baxter S, Callaway DJ, et al. (2010) A conformational switch in the scaffolding protein NHERF1 controls autoinhibition and complex formation. J Biol Chem 285: 9981-9994.

50. Ballif BA, Carey GR, Sunyaev SR, Gygi SP (2008) Large-scale identification and evolution indexing of tyrosine phosphorylation sites from murine brain. J Proteome Res 7: 311-318.

51. Zhang J, Petit CM, King DS, Lee AL (2011) Phosphorylation of a PDZ domain extension modulates binding affinity and interdomain interactions in postsynaptic density-95 (PSD-95) protein, a membrane-associated guanylate kinase (MAGUK). J Biol Chem 286: 41776-41785.

52. Niethammer M, Valtschanoff JG, Kapoor TM, Allison DW, Weinberg RJ, et al. (1998) CRIPT, a novel postsynaptic protein that binds to the third PDZ domain of PSD-95/SAP90. Neuron 20: 693-707.

53. Popovych N, Sun S, Ebright RH, Kalodimos CG (2006) Dynamically driven protein allostery. Nat Struct Mol Biol 13: 831-838.

54. Popovych N, Tzeng SR, Tonelli M, Ebright RH, Kalodimos CG (2009) Structural basis for cAMP-mediated allosteric control of the catabolite activator protein. Proc Natl Acad Sci U S A 106: 6927-6932.

55. Tzeng SR, Kalodimos CG (2009) Dynamic activation of an allosteric regulatory protein. Nature 462: 368-372.

56. Tzeng SR, Kalodimos CG (2012) Protein activity regulation by conformational entropy. Nature 488: 236-240.

57. Passner JM, Schultz SC, Steitz TA (2000) Modeling the cAMP-induced allosteric transition using the crystal structure of CAP-cAMP at 2.1 A resolution. J Mol Biol 304: 847-859.

58. Harman JG (2001) Allosteric regulation of the cAMP receptor protein. Biochim Biophys Acta 1547: 1-17.

59. Volkman BF, Lipson D, Wemmer DE, Kern D (2001) Two-state allosteric behavior in a single-domain signaling protein. Science 291: 2429-2433.

60. Li P, Martins IR, Amarasinghe GK, Rosen MK (2008) Internal dynamics control activation and activity of the autoinhibited Vav DH domain. Nat Struct Mol Biol 15: 613-618.

61. Yao X, Rosen MK, Gardner KH (2008) Estimation of the available free energy in a LOV2-J alpha photoswitch. Nat Chem Biol 4: 491-497.

62. Popovych N, Tzeng SR, Tonelli M, Ebright RH, Kalodimos CG (2009) Structural basis for cAMP-mediated allosteric control of the catabolite activator protein. Proc Natl Acad Sci U S A 106: 6927-6932.

63. Marlow MS, Dogan J, Frederick KK, Valentine KG, Wand AJ (2010) The role of conformational entropy in molecular recognition by calmodulin. Nat Chem Biol 6: 352-358.

64. Tzeng SR, Kalodimos CG (2011) Protein dynamics and allostery: an NMR view. Curr Opin Struct Biol 21: 62-67.

65. Akke M (2012) Conformational dynamics and thermodynamics of protein-ligand binding studied by NMR relaxation. Biochem Soc Trans 40: 419-423.

66. Sheppard D, Sprangers R, Tugarinov V (2010) Experimental approaches for NMR studies of side-chain dynamics in high-molecular-weight proteins. Prog Nucl Magn Reson Spectrosc 56: 1-45.